Electronic supplementary information

Fast solution-phase growth of centimeter-sized $Cs_3Cu_2X_5$ (X=Cl, I) single crystals for high-performance scintillators

Xiangshi Bin,‡[ab] Jiaxing Liu,‡[ab] Ruosheng Zeng,[a] Hongbang Liu,*[a] Jialong Zhao,*[a] Tao Lin*[ab]

a School of Physical Science and Technology, Laboratory of Optoelectronic Materials and Detection Technology, Guangxi Key Laboratory for Relativistic Astrophysics, Guangxi University, Nanning 530004, China

b Center on Nanoenergy Research, Guangxi University, Nanning 530004, China

*Correspondence: correspondence to E-mail: liuhb@gxu.edu.cn; zhaojl@ciomp.ac.cn; taolin@gxu.edu.cn;

‡These authors contribute equally to this work.

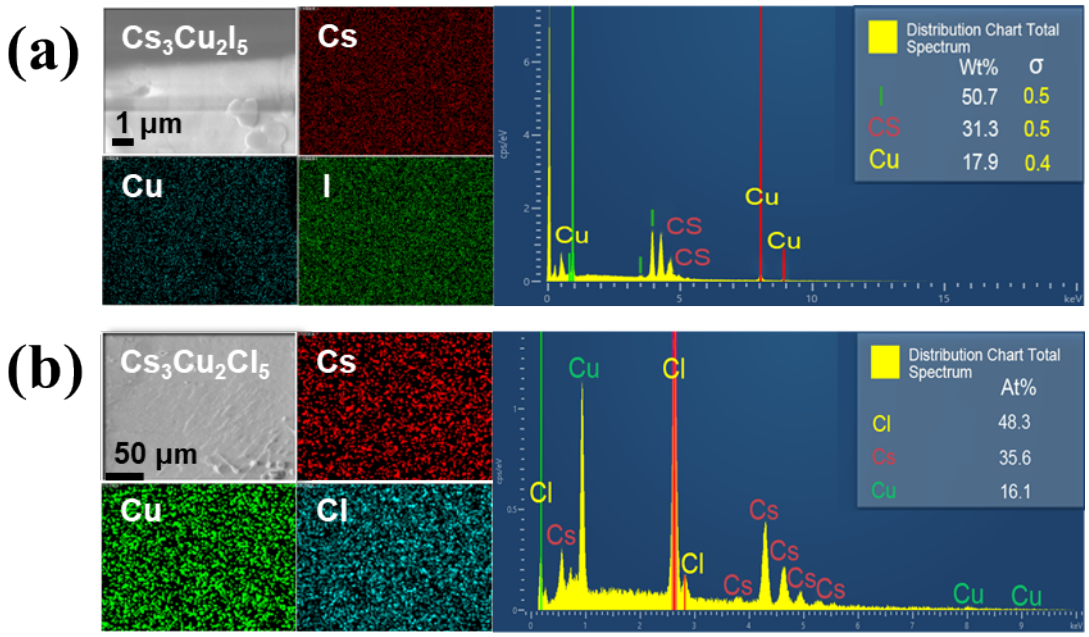

Fig. S1. SEM and EDS scans of (a) $Cs_3Cu_2Cl_5$ and (b) $Cs_3Cu_2I_5$ single crystals (SCs). The atomic ratios of Cs:Cu:Cl/I in both samples were close to 3:2:5.

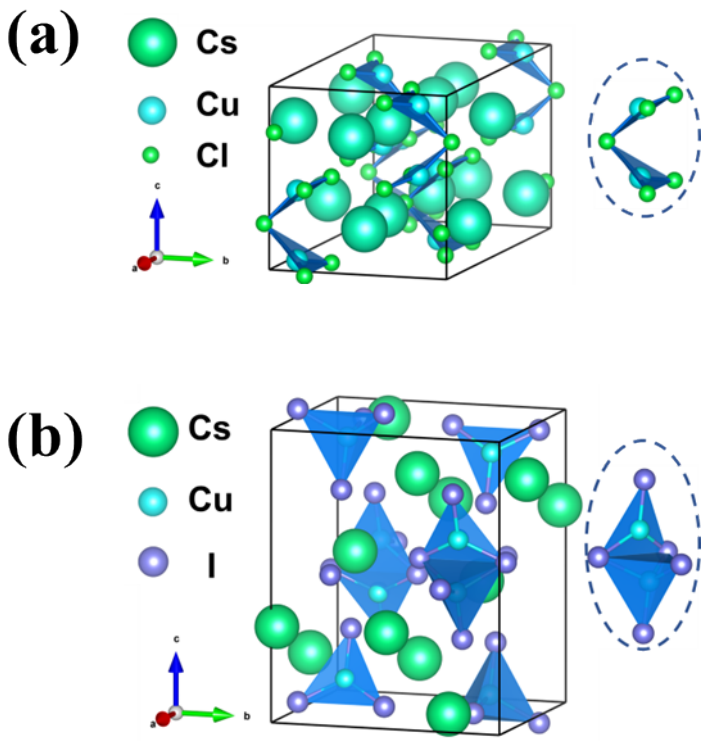

Fig. S2. (a) Crystal structure of $Cs_3Cu_2Cl_5$ SCs: The $[Cu_2Cl_5]^{3-}$ basic units in the unit cell contains two Cu^+ ions and five Cl^- ions. One Cu^+ ion coordinate with three Cl^- ions to forming a planar configuration. By sharing a Cl atom, two planes connect to create a folded $[Cu_2Cl_5]^{3-}$ dimer. These dimers are separated by large Cs^+ ions, resulting in a unique 0D structure. (b) Crystal structure of $Cs_3Cu_2I_5$ SCs: There are two sites for Cu^+ ions in one $[Cu_2I_5]^{3-}$ basic unit. In one site, the Cu^+ ion coordinates with three Cl^- ions, forming a planar triangle. In the other site, the Cu^+ ion coordinates with four Cl^- ions, forming a tetrahedron. These two geometries are connected by sharing two Cl^- ions, resulting in a complete $[Cu_2Cl_5]^{3-}$ unit. These $[Cu_2I_5]^{3-}$ basic units are separated by Cs^+ ions to from a 0D structure.

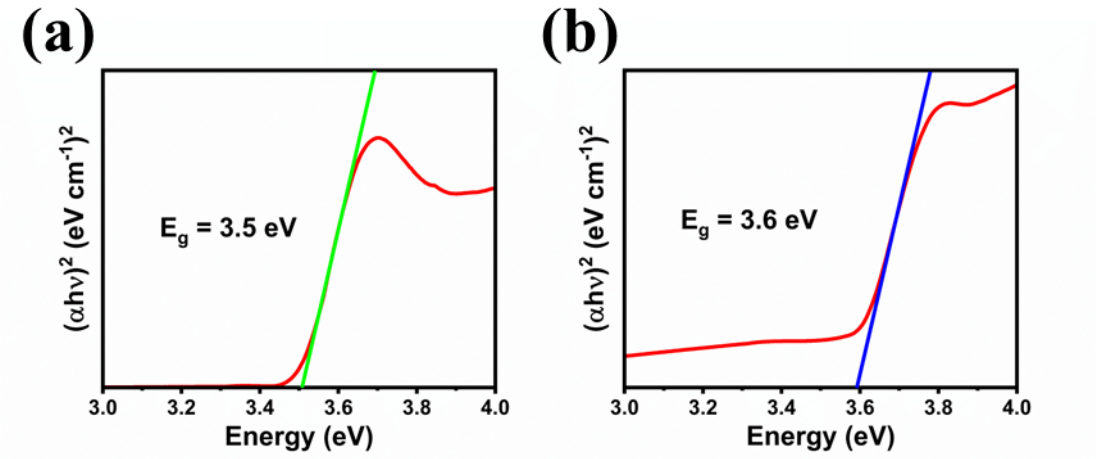

Fig. S3. Bandgaps of (a) $Cs_3Cu_2Cl_5$ SCs and (b) $Cs_3Cu_2I_5$ SCs as determined from Tauc plots.

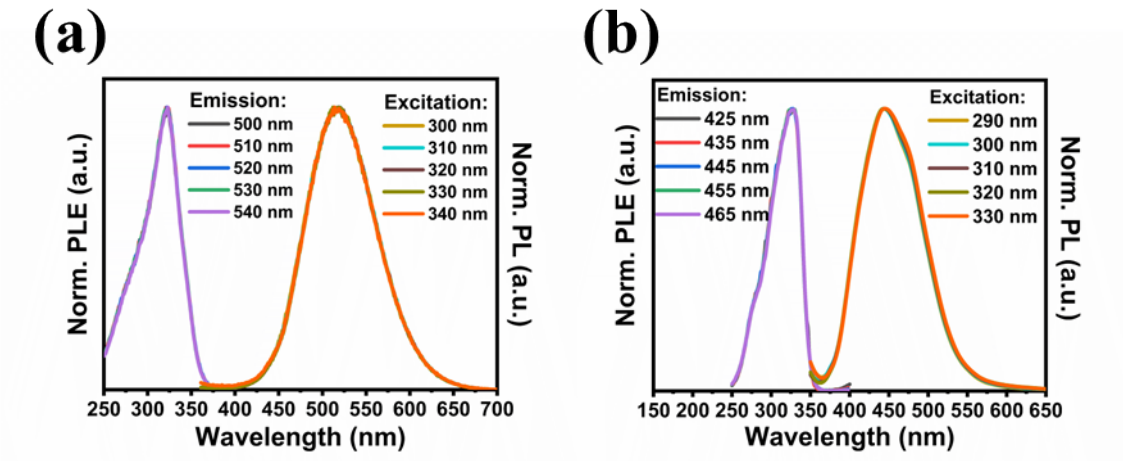

Fig. S4. The emission bands observed were approximately (a) 400 nm to 700 nm for $Cs_3Cu_2Cl_5$ and (b) 350 nm–650 nm for $Cs_3Cu_2I_5$. The positions and shapes of the emission bands remained consistent when the excitation wavelength was varied within a range covering the absorption edges. The excitation bands for each sample, covering a series of detecting wavelengths involved in the emission bands, showed the same position and shape.

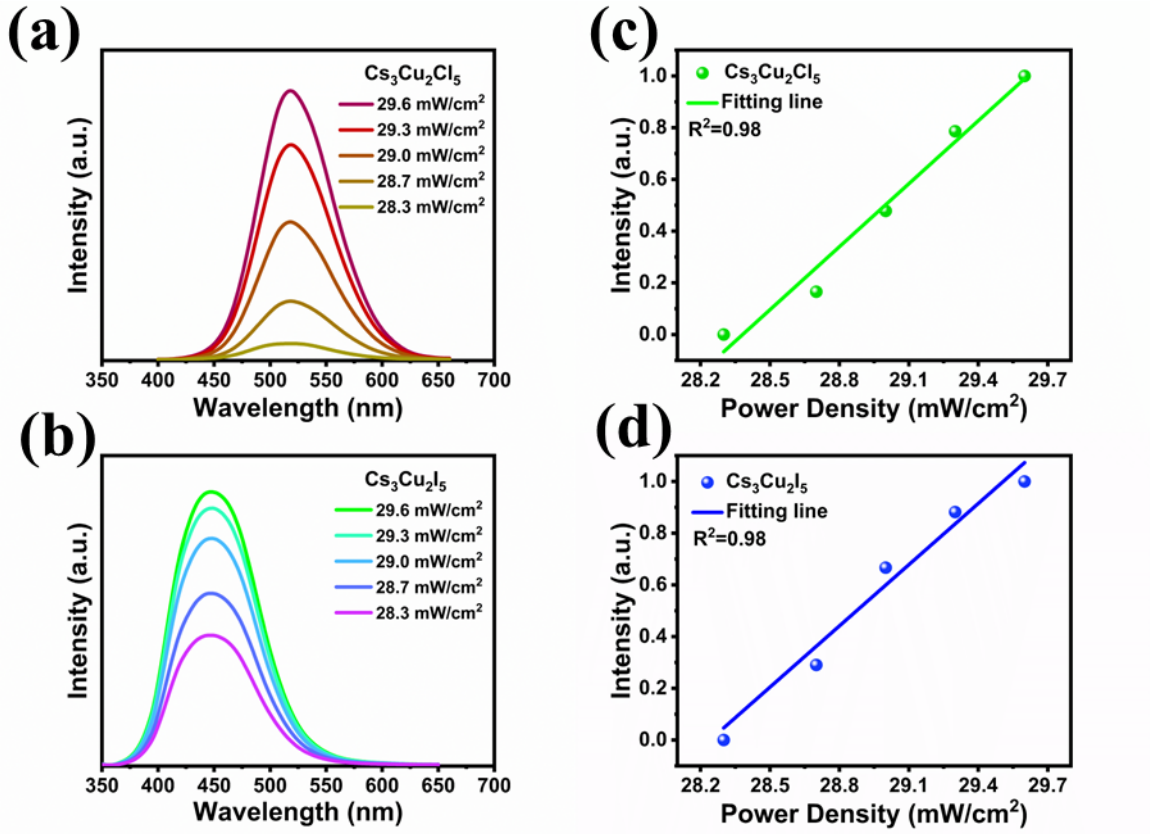

Fig. S5. PL spectra of (a) $Cs_3Cu_2Cl_5$ SCs and (b) $Cs_3Cu_2I_5$ SCs with variable power density, the clear signs of PL saturation under high-power excitation would be observed. (c) PL intensity increased linearly with the excitation power density of $Cs_3Cu_2Cl_5$ SCs and (d) $Cs_3Cu_2I_5$ SCs.

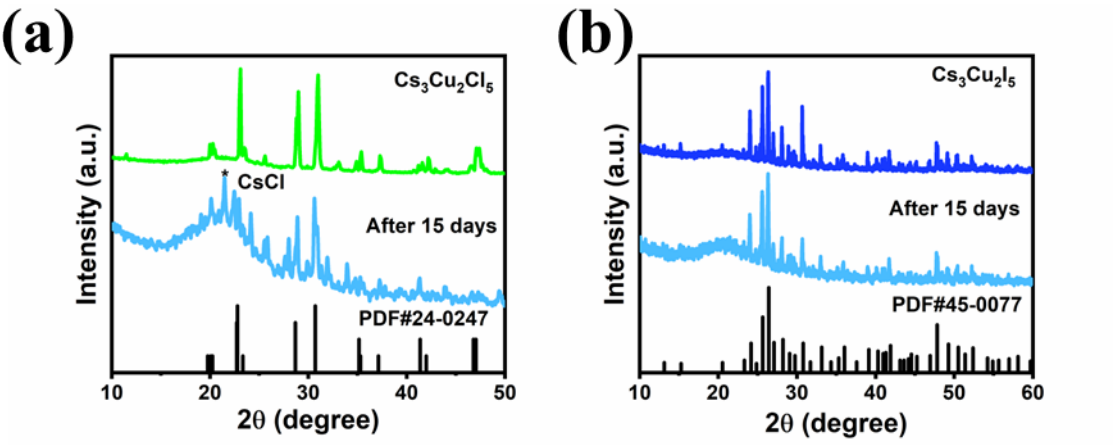

Fig. S6. XRD patterns of (a) $Cs_3Cu_2Cl_5$ and (b) $Cs_3Cu_2I_5$ including the as-prepared samples and ones exposed to air for 15 days. This RL quenching is primarily attributed to the decomposition of cesium-copper(I) halides, as a clearer phase ascribable to CsCl was observed in the $Cs_3Cu_2Cl_5$-PMMA sample.